

Pathological Characters and Molecular Pathogenesis of Diabetic Neuropathic Osteoarthropathy Cartilages Damage

Pei-Long Liu

Honghui Hospital of Xi'an Jiaotong University

Jia-Yu Diao

Shaanxi Provincial People's Hospital

Qiong Wang

Honghui Hospital of Xi'an Jiaotong University

Huan Liu

Xi'an Jiaotong University

Yan Zhang

Honghui Hospital of Xi'an Jiaotong University

Jing-Qi Liang

Honghui Hospital of Xi'an Jiaotong University

Feng Zhang

Xi'an Jiaotong University

Xiao-Jun Liang

Honghui Hospital of Xi'an Jiaotong University

HongMou Zhao (✉ zhao_hongmou@hotmail.com)

Honghui Hospital of Xi'an Jiaotong University <https://orcid.org/0000-0001-5760-9309>

Research Article

Keywords: diabetic neuropathic osteoarthropathy, pathological features, chondrocytes, RANKL/OPG, inflammation

Posted Date: October 18th, 2021

DOI: <https://doi.org/10.21203/rs.3.rs-969602/v1>

License:   This work is licensed under a Creative Commons Attribution 4.0 International License.

[Read Full License](#)

Abstract

Background: Diabetic neuropathic osteoarthropathy (DNOAP) is a rare and easily missed complication for diabetes that leads to increased morbidity and mortality. DNOAP is characterized by progressive destruction of bone and joint, but its pathogenesis remains elusive. We herein aimed to investigate the pathological features and pathogenesis of the cartilages damage in DNOAP patients.

Methods: The articular cartilages of 8 patients with DNOAP and 8 normal controls were included. Masson staining and safranin O/ fixed green staining (S-O) were used to observe the histopathological characteristics of cartilage, and the ultrastructural changes of chondrocytes were detected by electron microscopy. Chondrocyte were isolated from DNOAP group and control group. The expression of RANKL, OPG, IL-1 β , IL-6, TNF- α , Aggrecan protein were evaluated by Western blot. ROS levels were measured using a DCFH-DA probe. The percentage of apoptotic cells was determined by flow cytometry. The chondrocytes were cultured with different glucose concentrations to observe the expression of RANKL and OPG.

Results: Compared with the control group, the DNOAP group showed fewer chondrocytes, subchondral bone hyperplasia and structural disorder, and a large number of osteoclasts formed in the subchondral bone area. Moreover, mitochondrial and endoplasmic reticulum swelling were observed in the DNOAP chondrocytes. The chromatin was partially broken and concentrated at the edge of nuclear membrane. The ROS fluorescence intensity of chondrocyte in DNOAP group was higher than that in normal control group (28.1 ± 2.3 VS 11.9 ± 0.7 , $P < 0.05$). The expression of RANKL, TNF- α , IL-1 β and IL-6 protein in DNOAP group was higher than that in normal control group, while OPG and Aggrecan protein was lower than that in normal control group (both $P < 0.05$). Flow cytometry showed that the apoptotic rate of chondrocyte in DNOAP group was higher than that in normal control group ($P < 0.05$). The RANKL/OPG ratio showed significant upward trend when the concentration of glucose was over than 15mM.

Conclusions: DNOAP patients tend to have severe destruction of articular cartilage and collapse of organelle structure including mitochondrion and endoplasm reticulum. Indicators of bone metabolism (RANKL, OPG) and inflammatory cytokines (IL-1 β , IL-6 and TNF- α) play an important role in promoting the pathogenesis of DNOAP. The glucose concentration higher than 15mM made the RANKL / OPG ratio changed rapidly.

Introduction

Diabetic neuropathic osteoarthropathy (DNOAP) was first described in 1936 by Jordan. It is a serious complication of diabetes, accounting for 0.8-13.0% of all diabetic patients. And, the prevalence of high-risk patients can be as high as 29.0%^[1]. As diabetes mellitus has become one of the most common disorders now, there will be an increase in the prevalence of DNOAP. Patients with DNOAP often present with joint subluxations, dislocation, or pathological fractures, which reduce the quality of life and increase

the mortality significantly^[2, 3]. Accurate diagnosis and appropriate treatment could avoid the delays in patient condition and operation, improve clinical outcomes and lower the medical costs.

The pathogenesis of DNOAP, however, remains largely unknown. And, new prospects for studying DNOAP are constantly emerging. The investigation of DNOAP pointed out that inflammatory markers and the dynamics of bone metabolism were involved in the pathological process of it^[4-6]. Among them, the increase of pro-inflammatory cytokines tumor necrosis factor- α (TNF- α), interleukin-6 (IL-6) and IL-1 β in serum of DNOAP suffers has been reported multiple times^[4, 7]. In addition, Jeffcoate et al. proposed that the pathway of receptor-activator of nuclear factor kappaB (RANK), its ligand RANKL, and osteoprotegerin (OPG) played a role in disease progression of Charcot neuroarthropathy firstly in 2004^[8].

The RANKL/OPG axis is a key mediator which has been used to evaluate osteoclastogenesis and osteolytic processes in numerous diseases such as rheumatoid arthritis, osteoarthritis, and bone tumors. And the expression of RANKL was increased in diabetes caused by Oxidative stress and inflammation state^[9]. Furthermore, La Fontaine et al^[10] found that the number of bone trabeculae in patients with DNOAP was significantly reduced and the structure was disordered. However, there is no report on the pathological changes of cartilage from DNOAP patients.

In this study, articular cartilage specimens and chondrocytes were used to explore the pathological characteristics and molecular mechanism of DNOAP patients, to open novel avenues for clinical prevention and treatment.

Materials And Methods

Clinical samples

From March 2017 to June 2018, articular cartilage specimens were collected from 8 clinically confirmed DNOAP patients, and the articular cartilage of matched joints from 8 amputation patients without underlying disease were as control group.

Inclusion criteria for DNOAP patients are as follows: (1) DNOAP was definitely diagnosed according to the diabetes mellitus history, clinical and imaging manifestations, (2) Type I- IIIA according to Brodsky classification^[11], (3) Phase III judged by Eichenholtz classification system^[12], (4) patients underwent middle or posterior foot fusion surgery. Exclusion criteria: (1) Patients with peripheral arterial disease, (2) active infection and ulcer, (3) unclear diagnosis of DNOAP. The 8 patients with DNOAP were 3 males and 5 females, aged 20~66 (55.7 ± 3.8) years, diabetes mellitus duration of 6~14 (11.7 ± 3.1) years, DNOAP duration of 5~13 (7.3 ± 4.3) months. Two cases were Brodsky type I, 4 cases were type II, and 2 cases of Type IIIA.

Enrolled controls were patients without diabetes and peripheral neuropathy who underwent amputation due to traffic accident or serious trauma. Exclusion criteria: (1) osteoarthritis, Rheumatoid arthritis, and other degenerative joint disease, (2) open injury or contamination of affected joints. Eight cases of traffic

accident or severe injury amputation were recruited as the controls, including 4 males and 4 females, aged 19-65 (57.6 ± 3.7) years old.

The articular cartilages of tibiotalar joint, subtalar joint, and talonavicular joint were taken from two groups. The use of human samples was approved by the Ethical Committee of Honghui Hospital of Xi'an Jiaotong University (approval No.201702003), and informed consent was obtained from each participant.

Pathological examination

The articular cartilage biopsies from donors of DNOAP group and controls were fixed in 10% formaldehyde for 24 hours, decalcified by 15% neutral EDTA-2Na for 15 days, then dehydrated by alcohol gradient of different concentrations and embedded with paraffin. Cut the paraffin-embedded specimens into 5 μ m consecutively. Then, the tissue sections were stained with Masson's Trichrome Stain Kit and Modified Safranin O-Fast Green FCF Cartilage Stain Kit (Beijing Solarbio Science & Technology Co., Ltd), according to the manufacturer's instructions. Finally, the pathological changes of cartilage, calcified layer and subchondral bone were observed directly under the optical microscope.

Transmission Electron Microscopy

The fresh cartilage specimens of DNOAP group and controls were fixed with 2.5% glutaraldehyde at 4 °C in a volume of 1 mm³ overnight. Next day, the cartilage samples were rinsed with ddH₂O, fixed with 1% osmium acid for 1h, stained with 2% uranium acetate for 30min, dehydrated gradiently with 50%, 70%, 90%, 100% ethanol and 100% acetone. After infiltration, embedding and polymerization, the sections were sliced to a thickness of 70nm by ultramicrotome, and then stained with uranium acetate lead citrate. The ultrastructure of organelles in chondrocytes were observed under HITACHI H-7650 transmission electron microscope (Hitachi, Tokyo, Japan).

Chondrocyte maintenance

The cartilage samples were segmented into 3~5mm³ pieces, and washed into the phosphate buffer solution (PBS) containing penicillin (100U/L) and streptomycin (100mg/L). Then the small pieces were digested with 0.25% trypsin at room temperature for 15-20min, and centrifugated at 1000 \times g for 5min. After removing the supernatant, the deposit was washed with PBS for three times. Next, the deposit was digested at 37 °C for 8~10h with 0.2% Collagenase Type II (C2-BIOC, Millipore Sigma, USA) in a constant temperature shaker. After filtration by aseptic cell sieves, the cells were washed and collected through centrifugation (1000 \times g, 10 min). The chondrocytes were cultured with DMEM medium (Invitrogen, USA) supplemented with 10% fetal bovine serum (Thermo Fisher Scientific, USA) at 37°C in a humidified atmosphere containing 5% CO₂.

Detection of reactive oxygen species (ROS) in chondrocytes

Reactive oxygen species (ROS) production was detected with a Reactive Oxygen Species Assay Kit (Shanghai Beyotime Biotechnology Co., Ltd). Inoculate the chondrocytes into 6-well plate (1×10^6 cells per well) and 3 auxiliary holes were set for each group. When the cell fusion rate reached 70% ~ 80%, the culture medium was removed, and DCFH-DA with the concentration of $10 \mu\text{mol/L}$ was added into each well, and then the plate was placed in dark for 20min at 37°C . Wash the cells with serum-free DMEM for three times. ROS was measured by fluorescence microscope at an excitation wavelength of 485nm and an emission of 525nm. The intensity of each group was analyzed by Image Pro Plus image analysis software.

Western blotting

Protein concentration was detected using Pierce BCA Protein Assay Kit (Thermo Fisher Scientific, USA) in accordance with the manufacturer's instructions. Total proteins were electrophoretically separated on sodium dodecyl sulfate polyacrylamide gels (8-15%) according to the molecular size of the target protein, and were subsequently transferred onto polyvinylidene difluoride membranes. After being blocked with 5% skim milk, the membranes were incubated at 4°C overnight with the following primary antibodies: anti-RANKL, anti-OPG, anti-IL- 1β , anti-IL-6, anti-TNF- α and anti- β -actin (Proteintech, USA).

Then, the membranes were washed thoroughly and incubated with secondary antibodies (1:2000 anti-mouse/ rabbit, Santa Cruz Biotechnology, USA) at room temperature for 2 hours. The signals were visualized using the enhanced chemiluminescence method (Immobilon Western Chemiluminescent HRP Substrate, Millipore). The samples were analyzed in duplicate, and the experiment was performed three times.

Detection of apoptosis by flow cytometry

The percentage of apoptotic cells was ascertained through Annexin V/FITC-PI apoptosis detection kit (Beijing Sizhengbai Biotechnology Co., Ltd).

Cells were prepared with the concentration of $1 \times 10^6/\text{ml}$ in 10% bovine serum albumin, according to the manufacturer's instructions. After cultured in the incubator with 5% CO_2 at 37°C for 24h, the cells were collected in a 10 ml centrifuge tube, centrifuged at $1000 \times g$ for 5 min, and washed with precooled PBS twice. Added Annexin V-FITC/ PI and PI ($100 \mu\text{g}/\text{mL}$) working solution into cells, and stained for 15min at room temperature in dark. Flow cytometry was used to detect the apoptosis rate of cells, and Cell Quest software was used to obtain and analyze parameters. The experiment was repeated three times.

High glucose induced expression of RANKL and OPG in chondrocytes

Hyperglycemia is a common feature of DNAOP patients, thus, we simulated anomalous level of blood sugar *in vitro* by treating normal chondrocytes with a wide range of glucose concentrations (5mM, 10mM, 15mM, 20mM, 25 mM, 33mM) for 24 hours. Western blot analyses were used to detect the expression of RANKL and OPG in chondrocytes.

Statistical methods

Statistical analyses were performed with SPSS 19.0 (SPSS Inc., Chicago, IL, USA). Data from cell experiments were analyzed using unpaired Student's t-tests, and images based on the statistical analyses were made in GraphPad Prism 5.0 (GraphPad Software Inc, La Jolla, CA, USA). All hypothetical tests were two-sided, and *P*-values less than 0.05 were considered statistically significant in all tests.

Results

Histopathological characterization of articular cartilage

Changes in articular cartilage were explored under the optical microscope. In the articular cartilage from the control group, chondrocytes were in cartilage lacuna, cartilage matrix was stained evenly, and subchondral bone was arranged orderly (Fig. 1A,1B). However, in the tissues of DNOAP patients, S-O staining showed that the continuity of the superficial cartilage was interrupted, the vertical fracture entered the deep layer of cartilage. The chondrocytes around the fracture were rupture and the matrix was light stained. Subchondral bone plates and trabeculae were reduced, and osteoclasts aggregation was observed. The subchondral bone shows the characteristics of reactive bone and the structure is disordered (Fig. 1C). Masson's trichrome staining showed that hyaline cartilage was arranged in a cordlike arrangement, the chondrocytes and osteocytes were decreased. In addition, subchondral bone hyperplasia, structural disorder and cavities were observed (Fig. 1D). The histopathological findings of all DNAOP patients were consistent.

Ultrastructure of chondrocytes

The integrity of organelles is the primary condition for cellular homeostasis. Next, we observed the ultrastructure of chondrocytes by transmission electron microscope. In the normal chondrocytes, there were abundant rough endoplasmic reticulum and normal condensed chromatin in nucleus (Fig. 2A,2B). In the cells from DNOAP group, swollen mitochondria were found, some mitochondrial membranes were incomplete, and the arrangement of mitochondrial cristae was disordered. Furthermore, severe expansion of the endoplasmic reticulum and Golgi apparatus were scattered in the cytosol. The nucleus became larger, and the chromatin was partially broken, concentrated, and gathered at the edge of nuclear membrane (Fig. 2C, 2D).

Reactive oxygen species (ROS) increased in chondrocytes of the DNOAP group

Reactive oxygen species (ROS) are highly reactive molecules that provide the normal signals in various cell types. But the accumulation of ROS leads to oxidative damage of biomolecules, which further causes oxidative stress and even cell death. Thus, we detected the level of ROS in chondrocytes by fluorescence microscope, and found that the ROS fluorescence intensity of cells originated from DNOAP group was obviously higher than the cells from the controls (28.1 ± 2.3 vs. 11.9 ± 0.7 , $t = 19.059$, $P < 0.05$, Fig. 3)

Apoptosis increased in chondrocytes originated from DNOAP patients

We then compared the cell apoptosis between DNOAP group and the control group. Flow cytometry analysis demonstrated that the proportion of apoptotic chondrocytes was around 2.6 times higher in the DNOAP group than in the control group ($3.3 \pm 0.2\%$ vs. $1.2 \pm 0.1\%$, $P < 0.05$, Fig. 4).

The expression of RANKL, OPG, Aggrecan and inflammatory cytokines

Western blot analyses were performed on total protein extracted from articular cartilage specimens of DNOAP patients and control participants. It demonstrated that the tissues of DNOAP group expressed higher levels of RANKL, IL-1 β , IL-6 and TNF- α and lower levels of OPG and Aggrecan than that of normal group, respectively ($P < 0.05$, Fig.5). The comparison results of each pair of samples and age-matched controls were consistent. And representative images of each index detected in our study were shown in Fig.5.

High glucose induced the change of RANKL/OPG ratio in chondrocytes

Western blot analyses demonstrated that the expression of RANKL decreased slightly with glucose concentration increase of DMEM medium. However, a sharp decline in OPG was observed, and when the concentration of Glucose was or over than 20mM, the expression of OPG was almost undetectable. Then we found that the ratio of RANKL/OPG remained near 1:1 when the cells were cultured with 5mM glucose, but the ratio showed significant upward trend when the concentration of Glucose was over than 15mM. The ratio reached the peak at 20mM of Glucose, and then decreased slightly and almost remained at the same level (Fig.6).

Discussion

Neuroarthropathy, also known as Charcot's joint, refers to the progressive, painless and noninfective destructive disease of bone and joint caused by neuropathy. In 1886, Charcot first reported the bone and joint lesions of patients with spinal tuberculosis comprehensively. In 1936, Jordan found the relationship between diabetes and Neuroarthropathy, and proposed the concept of DNOAP for the first time^[13]. However, up to now, the pathogenesis of DNOAP have remained unclear. Limited previous studies focused on the changes of synovium and bone trabeculae. In this study, we detected the pathological changes of cartilage firstly.

There were a large number of chondrocytes disintegrated in the cartilage tissue of DNOAP patients, osteoclasts aggregation and subchondral bone remodeling in subchondral bone area. And all of the changes of cartilage above were not found in osteoarthritis or rheumatoid arthritis^[14]. Osteoclasts are closely related to bone resorption^[15]. Activation and aggregation of osteoclasts will cause bone resorption and destruction, and lead to development of DNOAP. In addition, we observed the ultrastructural features of chondrocytes originated from DNOAP patients with transmission electron microscope, and found mitochondrial swelling and disordered arrangement of mitochondrial cristae, and numerous vacuoles in the endoplasmic reticulum and Golgi. Moreover, the apoptotic rate of chondrocytes in DNOAP group was higher than that in control group. The activity of mitochondrial and endoplasmic

reticulum is closely related to the cell viability^[16]. Structural damage of mitochondria and endoplasmic reticulum will lead to the changes in cellular metabolism, even the programmed death of chondrocytes, namely apoptosis, and finally induced to the destruction of cartilage tissue structure and matrix.

ROS is the main substance that causes oxidative stress damage in tissues, which plays an important role in bone remodeling by stimulating RANKL and inhibiting OPG expression^[17, 18]. ROS had a negative effect on osteoblastic differentiation^[19]. On the contrary, osteoclast activity was directly stimulated by ROS^[20]. Verzijl et al. found that the deposition of advanced glycation end products (AGEs) and ROS were increased in chondrocytes exposed to high-glucose^[21]. Consistent with previous study, we found that the production of ROS in DNOAP chondrocytes was more than the healthy controls, accompanied by higher level of RANKL and lower of OPG. These findings suggested that ROS induced by hyperglycemia may stimulate osteoclast activation by regulating RANKL/OPG pathway in DNOAP patients.

RANKL/OPG system, as an important regulatory axis of bone turnover, plays an important role in the activation, aggregation and function of osteoclasts. RANKL belongs to the TNF superfamily and has the ability to promote osteoclast formation. Its main role is to activate the RANK, which regulates osteoclast differentiation, promotes osteoclastogenesis and bone resorption^[22]. OPG, the soluble decoy receptor of RANKL, is a cytokine synthesized by activated osteoblasts, commonly known as the “osteoclastogenesis inhibitory factor”. OPG antagonizes the RANKL-RANK interactions on the surfaces of osteoclast progenitors and blocks the resultant downstream osteoclastogenic cascade^[23]. In a nutshell, osteoclast activity is likely to depend, at least in part, on the relative balance of RANKL and OPG. In general, abnormal RANKL:OPG ratio predicts pathological states, and can lead to an uncontrolled loss of bone mass^[24, 25].

Under stable bone metabolism conditions, the secretion and expression of RANKL and OPG are dynamically balanced to maintain the homeostasis of osteogenesis and osteoclast. When the expression of RANKL increased and OPG decreased, osteoclasts would aggregate and activate, leading to bone destruction^[26, 27]. In the present study, we found that the expression of RANKL in DNOAP group was significantly higher than that in normal control group, while an opposite trend was observed for the OPG expression in two groups. These results suggested that the RANKL/OPG pathway may be involved in the pathological changes of cartilage in the patients with DNOAP. Previous studies failed to conclude the relationship between the RANKL/OPG pathway and the progression of DNOAP in peripheral blood^[4]. Thus, the change of RANKL and OPG expression in the local cartilage lesion would be a significant discovery in the study of DNOAP.

Abnormal inflammatory markers are a common feature in DNOAP patients^[28, 29]. Generally, pro-inflammatory cytokines regulate the inflammatory response, and have dynamic interactions with metabolites that could mediate the bone turnover^[30]. Kwan Tat et al. reported that the expression of RANKL was increased and OPG decreased in osteoarthritis chondrocytes under the stimulation of IL-1 β , TNF- α and PGE2^[31]. In our study, it was found that the expression of IL-1 β , IL-6 and TNF- α in DNOAP

chondrocytes was significantly higher than that in the control group. Previous researches have reached similar conclusions^[7, 32]. Therefore, we speculated that the effects of these inflammatory indicators on DNOAP may partly depend on the biochemical activation of the RANKL/OPG signaling pathway.

Persistent hyperglycemia is a common clinical manifestation in patients with DNOAP^[33]. We treated normal chondrocytes with glucose in different concentrations, and found that the expression of RANKL decreased slightly and OPG sharply with glucose concentration increase. Notably, RANKL/OPG ratio showed obvious upward trend when the concentration of Glucose was from 15mM to 20mM. Subsequently, the ratio decreased slightly and almost remained at the same level. Thus, the findings suggested that 15mM may be a threshold for the imbalance of chondrocyte metabolism, and may also be an important node that triggers the damage of cartilage and even the occurrence of DNOAP.

Conclusion

In this study, we reported the pathological features of cartilage and ultrastructural changes of chondrocytes in DNOAP patients for the first time. Indicators of bone metabolism (RANKL, OPG) and inflammatory cytokines (IL-1 β , IL-6 and TNF- α) play an important role in promoting the pathogenesis of DNOAP. The glucose concentration higher than 15mM made the RANKL / OPG ratio changed rapidly. These results settle a foundation for the further study on the pathogenesis of DNOAP. The broader involvement and clinical relevance of cartilage in the pathogenesis of DNOAP will be the focus of future investigations.

Abbreviations

AGEs: glycation end products, DNOAP, diabetic neuropathic osteoarthropathy, IL-1 β : interleukin-1 β , IL-6: interleukin-6, OPG: osteoprotegerin, RANK: receptor activator of nuclear factor $\kappa\beta$, RANKL: receptor activator of nuclear factor $\kappa\beta$ ligand, ROS: reactive oxygen species, S-O: safranin O/fixated green staining, TNF- α : tumor necrosis factor- α

Declarations

Acknowledgements

We are grateful to all the study participants for their contributions. We appreciate the entire data collection team.

Authors' contributions

ZHM conceived and designed the study. LPL, DJY, LH, LJQ performed all the experiments and assisted in data interpretation. ZY, LJQ, LXJ participated in the operation and collection of experimental specimens. ZHM and ZF supervised the study. LPL, DJY and WQ drafted the manuscript. All authors read and approved the final manuscript.

Funding

This work was supported by China postdoctoral science foundation funded project (2017M613178) and Shaanxi province natural science foundation project (2018JM7112)

Availability of data and materials

Not applicable.

Ethics approval and consent to participate

Permission to use the cartilage specimens from this study for research purposes was approved by the Ethical Committee of Honghui Hospital of Xi'an Jiaotong University (approval No.201702003), and all participants had provided written informed consent prior to surgery.

Consent for publication

Not applicable.

Competing interests

The authors declare that they have no competing interests.

Author details

¹ Foot and Ankle Surgery Department, Honghui Hospital of Xi'an Jiaotong University, No. 76 Nanguo Road, Xi'an 710054, People's Republic of China.

² Cardiovascular Department, Shaanxi Provincial People's Hospital, Xi'an 710068, People's Republic of China.

³ School of public health, Xi'an Jiaotong University, Xi'an 710086, People's Republic of China.

References

1. Zhao HM, Diao JY, Liang XJ, *et al.* Pathogenesis and potential relative risk factors of diabetic neuropathic osteoarthropathy [J]. *J Orthop Surg Res*, 2017, 12(1): 142.
2. Zakin E, Abrams R, Simpson DM. Diabetic Neuropathy [J]. *Semin Neurol*, 2019, 39(5): 560-569.
3. Kloska A, Korzon-Burakowska A, Malinowska M, *et al.* The role of genetic factors and monocyte-to-osteoclast differentiation in the pathogenesis of Charcot neuroarthropathy [J]. *Diabetes Res Clin Pract*, 2020, 166: 108337.
4. Yates TH, Cooperman SR, Shofler D, *et al.* Current concepts underlying the pathophysiology of acute Charcot neuroarthropathy in the diabetic foot and ankle [J]. *Expert Rev Clin Immunol*, 2020, 16(8): 839-845.

5. Mabileau G, Petrova N, Edmonds ME, *et al.* Number of circulating CD14-positive cells and the serum levels of TNF- α are raised in acute charcot foot [J]. *Diabetes Care*, 2011, 34(3): e33.
6. Folestad A, Ålund M, Asteberg S, *et al.* Role of Wnt/ β -catenin and RANKL/OPG in bone healing of diabetic Charcot arthropathy patients [J]. *Acta Orthop*, 2015, 86(4): 415-425.
7. Petrova NL, Petrov PK, Edmonds ME, *et al.* Inhibition of TNF- α Reverses the Pathological Resorption Pit Profile of Osteoclasts from Patients with Acute Charcot Osteoarthropathy [J]. *J Diabetes Res*, 2015, 2015: 917945.
8. Jeffcoate W. Vascular calcification and osteolysis in diabetic neuropathy-is RANK-L the missing link? [J]. *Diabetologia*, 2004, 47(9): 1488-1492.
9. Ng AYH, Li Z, Jones MM, *et al.* Regulator of G protein signaling 12 enhances osteoclastogenesis by suppressing Nrf2-dependent antioxidant proteins to promote the generation of reactive oxygen species [J]. *Elife*, 2019, 8.
10. La Fontaine J, Shibuya N, Sampson HW, *et al.* Trabecular quality and cellular characteristics of normal, diabetic, and charcot bone [J]. *J Foot Ankle Surg*, 2011, 50(6): 648-653.
11. Brodsky JW. The diabetic foot. In: Coughlin MJ, Mann RA, Saltzman CL, eds. *Surgery of the Foot and Ankle*. 8th ed. St Louis, MO, USA: Mosby, 2006:1281–1368.
12. Eichenholtz SN. *Charcot Joints*. Springfield, IL, USA: Charles C.Thomas, 1966.
13. Trieb K. The Charcot foot: pathophysiology, diagnosis and classification [J]. *Bone Joint J*, 2016, 98-b(9): 1155-1159.
14. Tateiwa D, Yoshikawa H, Kaito T. Cartilage and Bone Destruction in Arthritis: Pathogenesis and Treatment Strategy: A Literature Review [J]. *Cells*, 2019, 8(8).
15. Boyle WJ, Simonet WS, Lacey DL. Osteoclast differentiation and activation [J]. *Nature*, 2003, 423(6937): 337-342.
16. Zheng P, Chen Q, Tian X, *et al.* DNA damage triggers tubular endoplasmic reticulum extension to promote apoptosis by facilitating ER-mitochondria signaling [J]. *Cell Res*, 2018, 28(8): 833-854.
17. Baek KH, Oh KW, Lee WY, *et al.* Association of oxidative stress with postmenopausal osteoporosis and the effects of hydrogen peroxide on osteoclast formation in human bone marrow cell cultures [J]. *Calcif Tissue Int*, 2010, 87(3): 226-235.
18. Huang MS, Morony S, Lu J, *et al.* Atherogenic phospholipids attenuate osteogenic signaling by BMP-2 and parathyroid hormone in osteoblasts [J]. *J Biol Chem*, 2007, 282(29): 21237-21243.
19. Mody N, Parhami F, Sarafian TA, *et al.* Oxidative stress modulates osteoblastic differentiation of vascular and bone cells [J]. *Free Radic Biol Med*, 2001, 31(4): 509-519.
20. Key LL, Jr., Wolf WC, Gundberg CM, *et al.* Superoxide and bone resorption [J]. *Bone*, 1994, 15(4): 431-436.
21. Verzijl N, Bank RA, TeKoppele JM, *et al.* AGEing and osteoarthritis: a different perspective [J]. *Curr Opin Rheumatol*, 2003, 15(5): 616-622.

22. Myers DE, Collier FM, Minkin C, *et al.* Expression of functional RANK on mature rat and human osteoclasts [J]. *FEBS Lett*, 1999, 463(3): 295-300.
23. Harper E, Forde H, Davenport C, *et al.* Vascular calcification in type-2 diabetes and cardiovascular disease: Integrative roles for OPG, RANKL and TRAIL [J]. *Vascul Pharmacol*, 2016, 82: 30-40.
24. Boyce BF, Xing L. Biology of RANK, RANKL, and osteoprotegerin [J]. *Arthritis Res Ther*, 2007, 9 Suppl 1(Suppl 1): S1.
25. Mountzios G, Dimopoulos MA, Bamias A, *et al.* Abnormal bone remodeling process is due to an imbalance in the receptor activator of nuclear factor-kappaB ligand (RANKL)/osteoprotegerin (OPG) axis in patients with solid tumors metastatic to the skeleton [J]. *Acta Oncol*, 2007, 46(2): 221-229.
26. Deschner J, Wypasek E, Ferretti M, *et al.* Regulation of RANKL by biomechanical loading in fibrochondrocytes of meniscus [J]. *J Biomech*, 2006, 39(10): 1796-1803.
27. Chen YJ, Chan DC, Lan KC, *et al.* PPAR γ is involved in the hyperglycemia-induced inflammatory responses and collagen degradation in human chondrocytes and diabetic mouse cartilages [J]. *J Orthop Res*, 2015, 33(3): 373-381.
28. Petrova NL, Moniz C, Elias DA, *et al.* Is there a systemic inflammatory response in the acute charcot foot? [J]. *Diabetes Care*, 2007, 30(4): 997-998.
29. Hingsammer AM, Bauer D, Renner N, *et al.* Correlation of Systemic Inflammatory Markers With Radiographic Stages of Charcot Osteoarthropathy [J]. *Foot Ankle Int*, 2016, 37(9): 924-928.
30. Jeffcoate WJ, Game F, Cavanagh PR. The role of proinflammatory cytokines in the cause of neuropathic osteoarthropathy (acute Charcot foot) in diabetes [J]. *Lancet*, 2005, 366(9502): 2058-2061.
31. Kwan Tat S, Amiable N, Pelletier JP, *et al.* Modulation of OPG, RANK and RANKL by human chondrocytes and their implication during osteoarthritis [J]. *Rheumatology (Oxford)*, 2009, 48(12): 1482-1490.
32. Petrova NL, Dew TK, Musto RL, *et al.* Inflammatory and bone turnover markers in a cross-sectional and prospective study of acute Charcot osteoarthropathy [J]. *Diabet Med*, 2015, 32(2): 267-273.
33. Johnson-Lynn SE, McCaskie AW, Coll AP, *et al.* Neuroarthropathy in diabetes: pathogenesis of Charcot arthropathy [J]. *Bone Joint Res*, 2018, 7(5): 373-378.

Figures

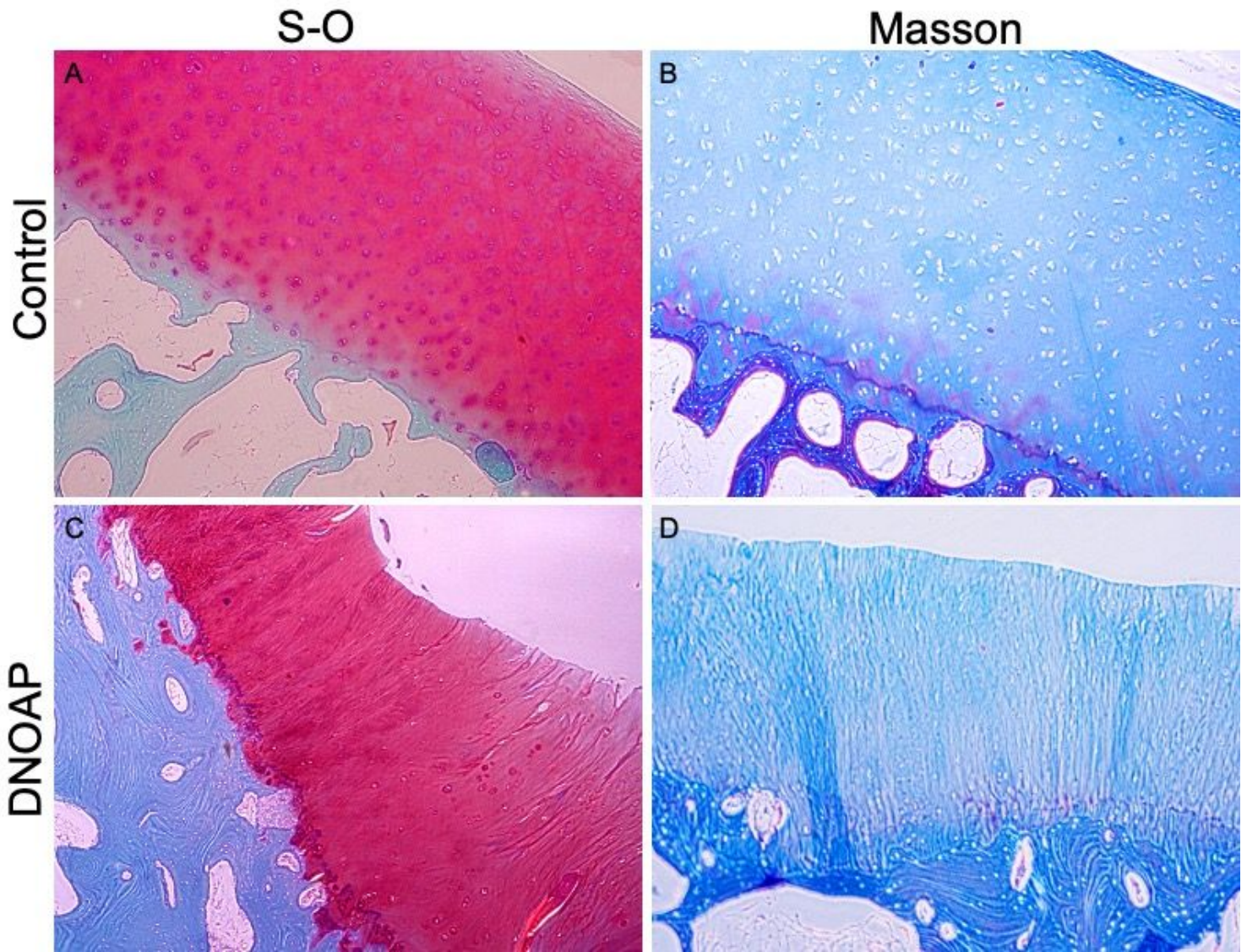


Figure 1

Pathological changes of cartilage in each group under S-O staining and Masson staining (100×). Representative S-O staining of cartilage in the control group (A) and DNOAP group (B). Representative Masson staining of cartilage in the control group (C) and DNOAP group (D). S-O, Modified Safranin O-Fast Green FCF Cartilage Stain, Masson, Masson's Trichrome Stain.

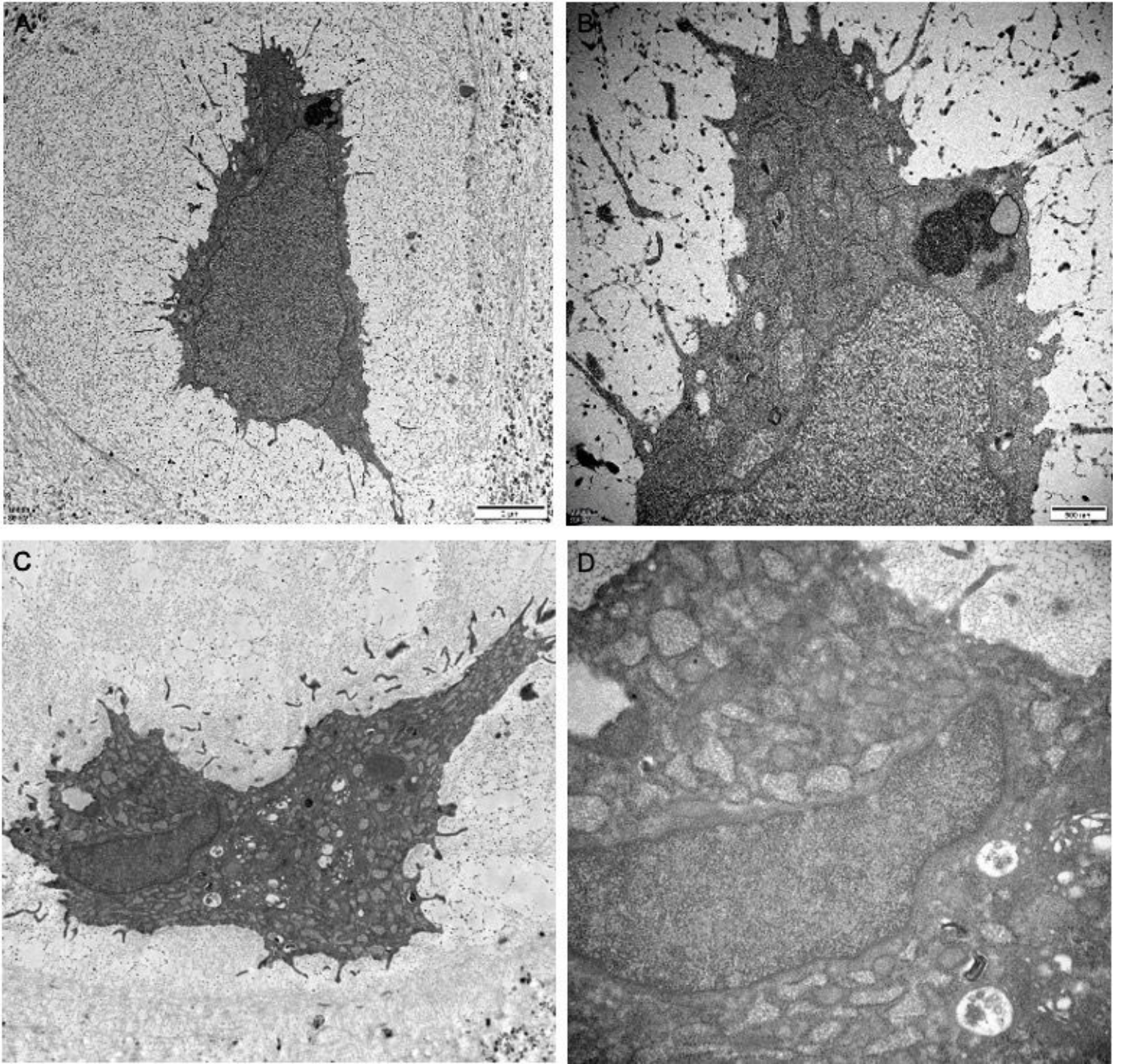


Figure 2

Ultrastructure of chondrocytes in each group under transmission electron microscope. The morphology of organelles in chondrocytes of control subjects (A, B). The morphology of organelles in chondrocytes of DNOAP patients (C, D). The magnification of A/C were 1×10^4 times, and B/D were 3×10^4 times.

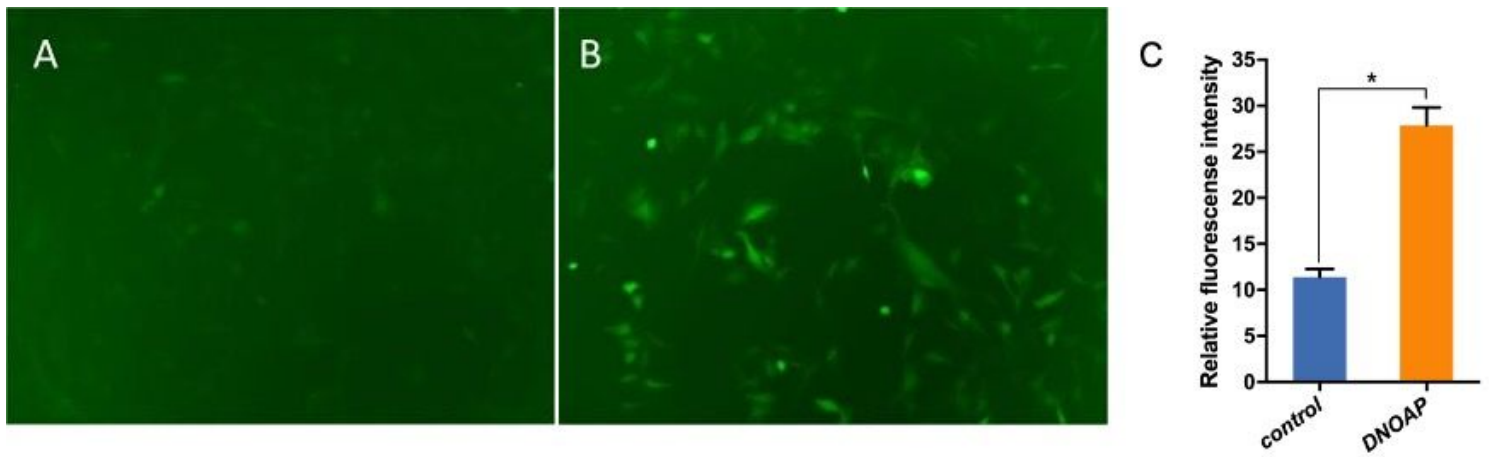


Figure 3

The level of ROS increased in chondrocytes of the DNOAP group. Representative images were taken in control group (A) and DNOAP group (B) via fluorescence microscope ($\times 100$). (C) The result depicts the comparative analysis of ROS levels in chondrocytes of two groups. The error bars presented as mean \pm Standard Error of Mean (SEM) with analysis of unpaired Student's t-test. *P < 0.05, compared with control group.

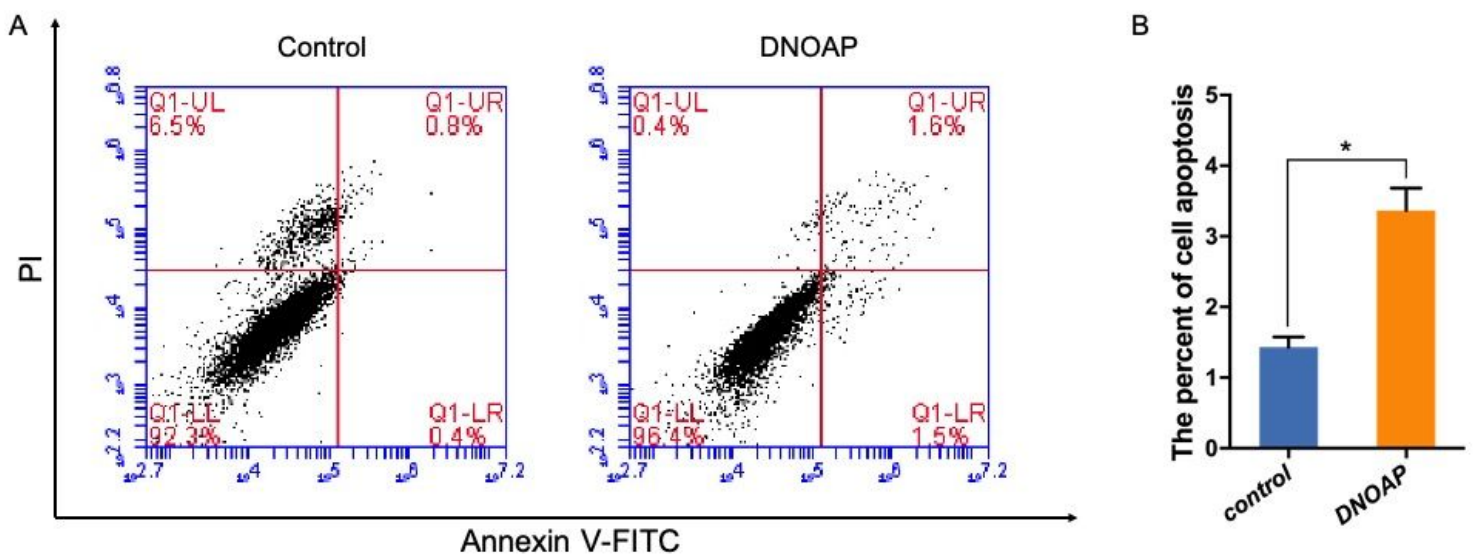


Figure 4

The percentage of apoptotic chondrocytes increased in the DNOAP group. (A) Representative images of flow cytometry (FCM) using Annexin V-FITC and PI staining. (B) Column bar graph showing a dramatically bigger early and late apoptosis ratio in cells of DNOAP patients than the controls. Each group was independently repeated three times, 3000 cells were calculated. The error bars presented as mean \pm Standard Error of Mean (SEM) with analysis of unpaired Student's t-test. *P < 0.05, compared with control group.

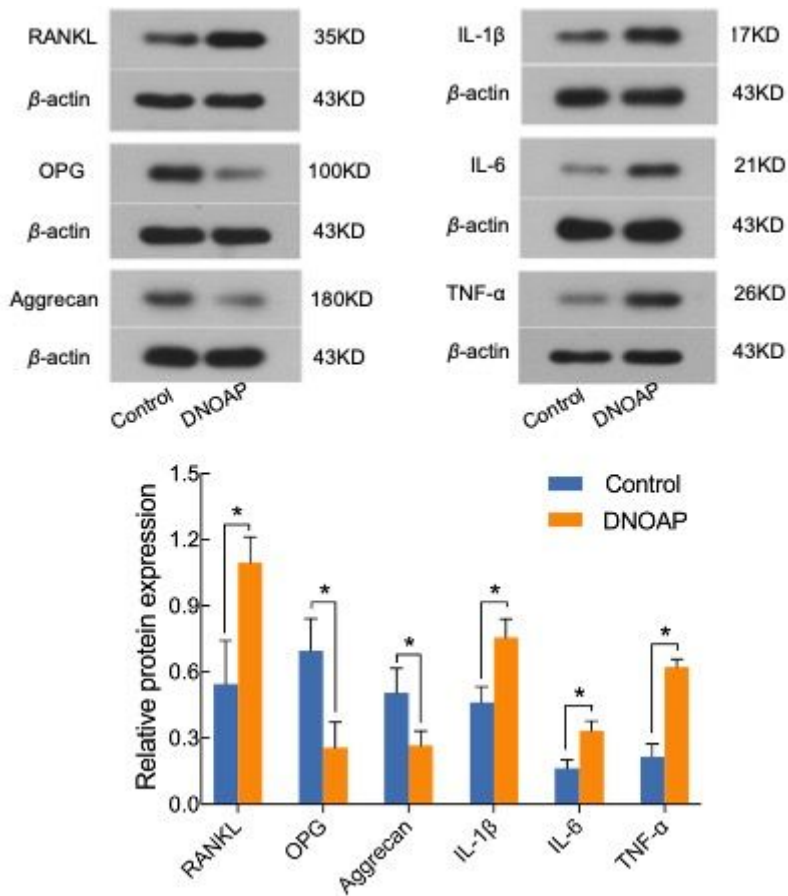


Figure 5

The protein expression of RANKL, OPG, Aggrecan, IL-1β, IL-6 and TNF-α in cartilage specimens of DNOAP and control group. Representative western blot bands and analysis in samples of DNOAP and control group. β-actin was used as a reference for calculating the relative protein expression. The error bars presented as mean ± Standard Error of Mean (SEM) with analysis of unpaired Student's t-test. *P < 0.05, compared with control group.

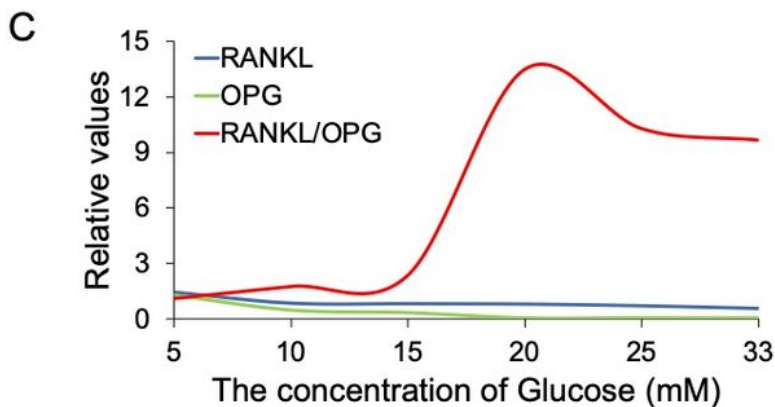
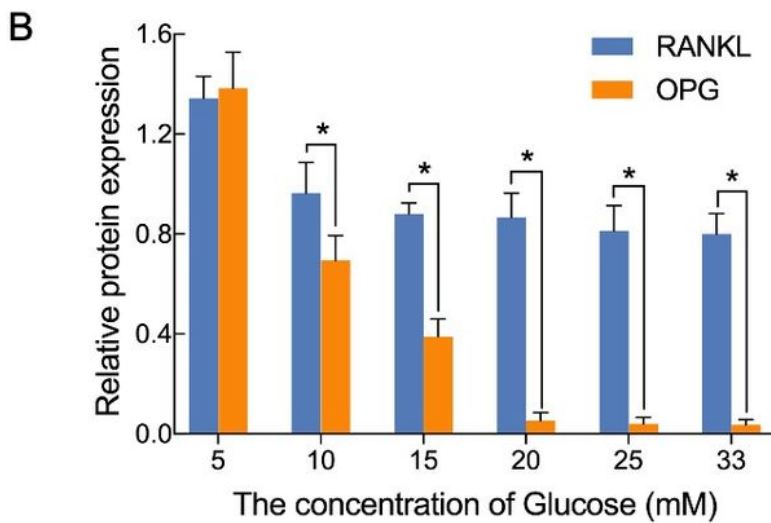
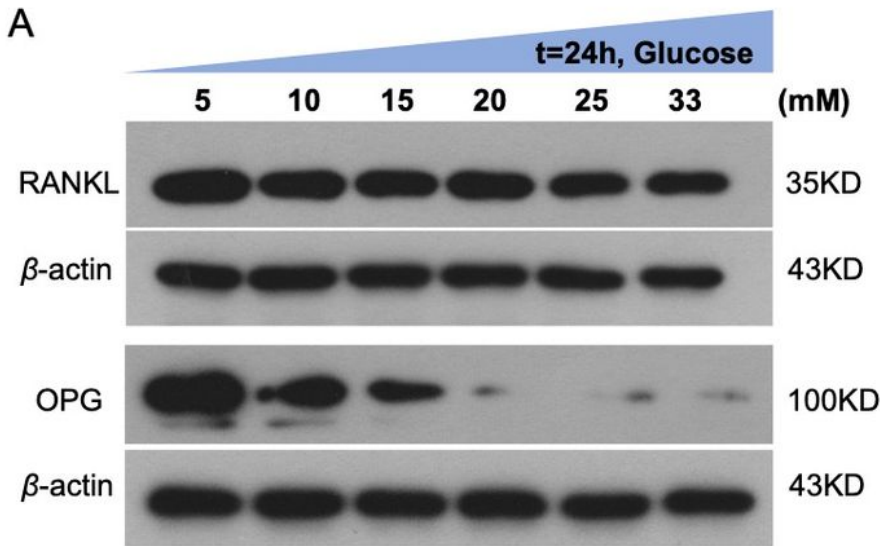


Figure 6

The expression of RANKL, OPG and RANKL-OPG ratio changed under various concentration of glucose. Representative western blot bands(A) and analysis (B, C) of RANKL, OPG in chondrocytes under different concentration of glucose. β -actin was used as a reference for calculating the relative protein expression. Each group was repeated at least three times. The error bars presented as mean \pm Standard Error of Mean (SEM) with analysis of unpaired Student's t-test. * $P < 0.05$, compared with the control group.